NASA CONTRACTOR REPORT

NASA CR-375

SOME STUDIES OF NONLINEAR LATERAL SLOSHING IN RIGID CONTAINERS

by H. Norman Abramson, Wen-Hwa Chu, and Daniel D. Kana

Prepared under Contract No. NASr-94(03) *by*
SOUTHWEST RESEARCH INSTITUTE
San Antonio, Texas
for

NATIONAL AERONAUTICS AND SPACE ADMINISTRATION • WASHINGTON, D. C. • JANUARY 1966

SOME STUDIES OF NONLINEAR LATERAL SLOSHING IN RIGID CONTAINERS

By H. Norman Abramson, Wen-Hwa Chu,
and Daniel D. Kana

Prepared under Contract No. NASr-94(03) by
SOUTHWEST RESEARCH INSTITUTE
San Antonio, Texas

for

NATIONAL AERONAUTICS AND SPACE ADMINISTRATION

For sale by the Clearinghouse for Federal Scientific and Technical Information
Springfield, Virginia 22151 – Price $2.00

ABSTRACT

Some experimental data, primarily on total force response, are presented for nonlinear lateral sloshing in rigid tanks of various geometries. Some effect of excitation amplitude on liquid swirl boundaries in an open circular cylindrical tank is noted. Data for the circular cylindrical tank is also compared with theoretical predictions. The primary nonlinear effects observed in all tanks were decreasing response frequency with increasing excitation amplitude and jump phenomena.

INTRODUCTION

The linearized theory of lateral sloshing of liquids in rigid containers is now well established and its application in design procedures is routine. Nonetheless, nonlinearities in the amplitude-frequency response of liquids in containers of various geometries have long been noted (1), although little quantitative data has been published. For example, it is evident that even in a circular cylindrical tank undergoing lateral excitation, the liquid free surface will form into a large amplitude breaking wave as the neighborhood of each of its natural resonant frequencies is approached, with obvious strongly nonlinear effects (see Fig. 1). In fact, in this particular instance, the situation then becomes even more complex as the liquid free surface takes on new modes of motion, arising primarily from these nonlinearities, and described variously as "rotary sloshing" or "swirl" (2, 3).

Significant nonlinearities have been observed also in spherical tanks (4), sector compartmented circular cylindrical tanks (5, 6), and in long rectangular tanks in pitch (7). Of course, the liquid response will exhibit significant nonlinearities in a tank of almost any geometry if the excitation amplitude is sufficiently large, or if mechanical baffling devices are introduced in the tank so as to provide very large amounts of damping. The circular cylindrical tank compartmented into sectors seems to be particularly sensitive to excitation amplitude, as shown in Figure 2, with

some dependence of liquid natural frequency on excitation amplitude down to even quite small values (6). Inasmuch as large rocket boosters are currently being designed with sector compartmented cylindrical tanks, such nonlinearities may have extremely important consequences for both control system and structural design.

Vertical or longitudinal excitation of cylindrical tanks also leads to interesting nonlinear motions of the liquid free surface (8). Large amplitude free surface motions occur when the liquid responds as a one-half subharmonic of the excitation and 'jump' phenomena are exhibited, as is common to nonlinear systems.

Some laboratory investigations of interactions between contained liquids and thin-walled elastic shells have also revealed interesting nonlinear phenomena (9, 10). The simple presence of the liquid free surface in such an elastic shell leads to some nonlinearity in the shell wall response but, even more startling, under certain circumstances a high frequency small amplitude vibrational excitation of the elastic wall in a circumferential mode may couple with the liquid and lead to a low frequency large amplitude free surface motion of the liquid in a rotationally symmetric mode! Attempts to describe this phenomenon analytically or to predict its occurrence have thus far proven fruitless, partially because of the extreme difficulties arising from the governing nonlinear effects whose fundamental nature even are very poorly defined. The nonlinear aspects of large amplitude liquid

motions arising essentially from subharmonic response in both antisymmetric and symmetric modes during vertical excitation are the subject of another program of investigation (8); however, little information is available concerning large amplitude antisymmetric modes more typical of lateral sloshing. In any event, it is clear that much remains to be learned concerning nonlinear liquid behavior, and therefore it is for this reason that the work reported in this paper was undertaken. Even though the results reported are not yet sufficient to enable us to explain the coupling and the characteristics of the response of both liquid and elastic shell that have been observed, it is hoped that the data that have been obtained will at least assist in defining better some of the fundamental aspects of nonlinear lateral sloshing in rigid containers.

EXPERIMENTAL APPARATUS AND INSTRUMENTATION

The apparatus employed in the present study of lateral sloshing in rigid tanks is shown overall in Figure 3, while closeup views of cylindrical and spherical tanks mounted in the apparatus are shown in Figure 4. Essentially, this set-up is similar to the large SwRI slosh facility which has been employed in many previous experimental studies of sloshing (11); however, in view of the fact that nonlinear aspects of lateral sloshing were to be investigated in the present effort, the apparatus was designed to permit considerably more precise and varied experimental observations than were possible with the original facility.

As is seen in Figure 3, the apparatus consists of (a) a massive base supporting all components of the system, (b) a carriage which may be excited either in translation or in pitching and which in turn supports the test tank, (c) an electrodynamic vibration exciter, and (d) an instrumentation system. The carriage is suspended from a sub-base by four tension springs to sustain its weight and is guided in an accurate linear motion by four steel shafts sliding in teflon bearings mounted on the base. This arrangement, shown in Figures 3 and 4, is for translational excitation, with some slight modifications being required for pitching excitation.

Circular cylindrical and spherical test tanks having inside diameters of 7.70 in. and 7.60 in., respectively, and fabricated from lucite plastic

were employed in this program, with water as the sloshing liquid. The tanks were mounted to the carriage by four very stiff, yet sensitive, strain-gaged force links; these are similar in principle to those employed on our larger and older facility (11) except that they are provided with strain sensing elements both parallel and normal to the direction of excitation. This part of the instrumentation system is thus designed to provide the capability for measuring both components of the total force and moment exerted on the tank by the sloshing liquid. The inertia signal of the empty tank is automatically subtracted from the output signals of the force and moment bridges by employing an inertial balancing device. This consists basically of two accelerometers that are considerably more sensitive than are the force links and mounted so as to experience the same acceleration as the tank, with their output signal wired to oppose that of the empty tank in the main force link bridge. Exact cancellation can be accomplished so that the resultant signal obtained represents only the total reaction force or moment of the liquid on the tank. The high stiffness of the tank support mounts is assurance that the motion of the test tank is essentially that of the carriage; the use of semiconductor strain gages as sensing elements in the stiff mount nonetheless provides a very sensitive monitoring system.

A 50# force output electrodynamic vibration exciter was employed to provide an accurate and noise-free power source, at frequencies above about 1.5 cps. The displacement input was monitored by means of strain

gages mounted on flexures supporting the shaker armature. The frequency of this displacement signal was accurately measured on an electronic counter so that various amplitudes and frequencies of the carriage (and tank) displacement could readily be adjusted at the shaker console. Additionally, a simple servo-system was utilized to provide automatic constant amplitude control of displacement as frequency was varied.

Up to six liquid wave height transducers could be employed in the cylindrical tank to observe liquid free surface displacement at various points over the tank cross section. These transducers are of the resistive Wheatstone bridge type (12) that have been previously employed in similar studies (8). Each transducer can provide the time variation of liquid height at a specific point in the tank, and thus the liquid mode shapes can be readily determined.

Each channel of instrumentation from the entire experimental apparatus consists of some arrangement of Wheatstone bridge powered by a corresponding channel of a CEC carrier amplifier unit, with these outputs then recorded on a CEC chart recorder.

EXPERIMENTAL RESULTS

The tank configurations investigated during the course of this program were circular cylindrical, 90° sector cylindrical, and spherical. The basic objective of the experiments was, of course, to provide quantitative data regarding the fundamental aspects of nonlinear lateral sloshing in rigid containers; therefore, attempts were made to measure both liquid free surface displacements and total forces. Because of the well-known occurrence of swirl modes near the liquid natural frequencies (2, 3), the circular cylindrical tank and the spherical tank were also investigated with vertical splitter plates installed parallel to the direction of excitation to suppress rotational motions and thus the onset of swirl. The data obtained for each of the tank configurations are discussed in detail below.

Circular Cylindrical Tank

Data were first obtained for the open circular cylindrical tank (i.e., no vertical splitter plate) at a liquid depth of $h/d = 1.0$. Liquid amplitude responses in the first antisymmetric slosh mode are shown as a function of excitation frequency, for several constant values of excitation amplitude X_o/d, in Figure 5. The average liquid surface displacement at the wall a_o/d has been utilized for convenience since the actual upward displacement from the mean liquid level is usually greater than the downward displacement, in this mode. The average amplitude, as employed here, is

one-half of the peak-to-peak amplitude value measured near the wall, in line with the axis of excitation.

Most of the data shown in Figure 5 were obtained by maintaining constant excitation amplitude while varying excitation frequency. At first, data were taken only for liquid motions arising basically from the first antisymmetric slosh mode, with no swirl occurring. Subsequently, the boundary of the swirl region was defined experimentally by maintaining constant excitation frequency and slowly increasing excitation amplitude until the swirl motion began to appear. The onset of swirl could be determined relatively precisely not only by visual observation but by the appearance of a significant force normal to the direction of excitation on the oscillograph output. The swirl boundary thus obtained is shown in Figure 5. It should be noted that this boundary is dependent upon both excitation frequency and amplitude since in certain instances it was found that large amplitude breaking waves could be produced without swirl. In addition, it should be noted that within the swirl region the motion of the liquid has a phase angle of near 90° with respect to the input displacement. Finally, it is worth pointing out again that this mode of liquid behavior is now rather well understood analytically, with good experimental correlation for very small excitation amplitudes (2, 3); the data presented here in Figure 5 are intended primarily to show the essential effects of increasing excitation amplitudes.

It has customarily been thought that the first antisymmetric slosh mode is characterized only by a rocking motion of an essentially planar surface, departing from this only at relatively large excitation amplitudes. However, several instances of anomalous behavior were observed during these tests, even at quite low values of excitation amplitude. For example, during one test run with $\omega^2 d/g = 2.00$ and $X_o/d = 0.005$ the surface displacement was recorded in some detail by means of the six liquid height transducers described earlier. The liquid surface was found to consist of a combination of two basic modes, the first antisymmetric mode at the frequency of excitation (1.6 cps) and the first symmetric mode occurring as a superharmonic at double the frequency of excitation. The antisymmetric component lagged the symmetric component significantly. A normalized plot of these two components is shown in Figure 6. While studies of liquid motions in longitudinally (vertically) excited tanks have revealed that both subharmonic and superharmonic liquid modes occur in abundance (8), it is believed that this is the first time that any such observation has been made in lateral sloshing.

Figure 7 shows dimensionless force amplitude (in the direction of excitation) corresponding to the liquid surface displacement data of Figure 5. The swirl boundary has not been so well defined in this instance as before.

Half-Cylindrical Tank

In an attempt to avoid the complexities introduced by the occurrence of the liquid swirl mode, the circular cylindrical tank was modified by the

installation of a vertical splitter plate parallel to the direction of excitation. This proved to be a very effective manner in which to suppress swirl, and therefore the complete liquid displacement response curve could be determined, as shown typically in Figure 8. Even at the quite small value of excitation amplitude employed for this particular piece of data, the nonlinear softening characteristic jump phenomenon is clearly demonstrated.

Total force response data (in the direction of excitation) are shown in Figure 9 for several values of excitation amplitude; corresponding phase angle data are shown in Figure 10. All of these data ere obtained by varying frequency while maintaining constant excitation amplitude; the sweep in frequency was made by first starting at a very low value and slowly increasing until substantially above first mode resonance, and then sweeping back down to low values. This procedure revealed jump phenomena very clearly. The nonlinear softening characteristic of the response curves of Figure 9 is quite evident.

The phase angle data given in Figure 10 are really not very satisfactory, but are included here in the interest of completeness. Figure 10a shows leading phase angles in the frequency range below resonance; this is believed to occur solely as the result of certain deficiencies in the instrumentation, and therefore similar lead angles in this frequency range in Figures 10b and 10c were arbitrarily changed to zero values. Similarly, the out-of-phase data do not come to 180°, nor do the jumps occur in the

vicinity of 90°; it would appear that a consistent error of about 15° - 20° is present in all of these phase angle data*.

The experimentally determined total force data are also compared directly with some theoretical predictions in Figure 9. The calculations result from extensions of the analysis of Hutton (3)**. This theory is basically one of third order but even then accounts for only certain elements of the nonlinear aspects of the problem; nevertheless, the theory is quite complex in its analytical details and consequently good agreement with experimental data at and beyond resonance is hardly to be expected. If one were to require the development of an improved theory, the choice between recommending a 'better' third-order theory or a similar fifth-order theory would not be an easy one. In any event, it may be noted from Figure 9 that the agreement between theory and experiment for the in-phase branches is rather good, for all four values of excitation amplitude. The agreement is not so good for the out-of-phase branches. In the vicinity of resonance the theory departs rather widely from the experimental values and, except in Figure 9a where the excitation amplitude has the smallest value, does not give a good value for the frequency at which the jump occurs.

* A somewhat different arrangement of instrumentation employed with the open circular cylindrical tank always gave zero phase angle in this region, as should be the case; the vertical splitter plate could not have caused such shifts in phase angle without also causing changes in total force (compare with data of Fig. 7).

**A review of the basic theory (3) and the results of the extended analysis are given in the following section of this report.

90° Sector Cylindrical Tank

While significant variations in the value of the lowest liquid resonant frequency as a function of excitation amplitude in sector compartmented cylindrical tanks had previously been noted [see (5), (6) and Fig. 2], it was felt that some study of large amplitude forced response might be of interest. Accordingly, a quarter-tank (90° sectors) was employed to produce the data shown in Figures 11 and 12. Again, the phase angle data of Figure 12 are not good but are included for completeness.

The total force response data given in Figure 11 were obtained by slowly sweeping frequency with constant excitation amplitude, as before. As is well known (5, 6) sector compartmented tanks exhibit liquid resonances in sets, corresponding to the orientation of the various sectors with respect to the direction of the excitation. For the 90° sector tank, the two lateral sectors respond at the lower frequency and the fore and aft sectors at a somewhat higher value of frequency. Thus, the forced response curves will exhibit two resonant peaks (5). Looking at the response curves of Figure 11, however, reveals other interesting features as well; for example, double jumps occur with each resonant peak, but both are downward from higher to lower amplitudes*. This arises, of course, from the fact that the data represent the total force response of all four sectors, even though

*This interesting effect was not observed in (5) because of the limitation to very small excitation amplitudes in that work.

only two of these are near resonance, and as a result there is some modification of the customary response picture. The individual pairs of sectors do, of course, have general response characteristics that are more typical of what we have already seen for the full cylindrical tank (at very small values of excitation amplitude); for increasing frequency, the jump up in amplitude occurs in the lateral sectors at 2.68 cps and in the fore and aft sectors at 3.0 cps, while the jump down in amplitude for decreasing frequency occurs at 2.91 cps for the fore and aft sectors and at 2.59 cps for the lateral sectors.

Therefore, in summary, it is seen that each pair of sectors have total force and phase response similar in form to those of the full cylindrical tank, but the two sector pairs resonate at somewhat different frequencies so that the magnitude of the total resultant force gives the response data shown in Figure 11. All jumps then occur downward to lower force amplitudes, and total phase angles are also correspondingly altered. Figure 11a also shows the total force response of an equivalent "frozen" liquid mass; in this instance, the phasing of the forces produced by the various sectors at the higher frequencies tends to cancel and produce an even lower total force than does the equivalent frozen mass.

Spherical Tank

As in the case of the circular cylindrical tank, it was found necessary to install a vertical splitter plate in the spherical tank parallel to the direction of excitation) in order to suppress the liquid swirl mode.

Resulting total force response data (amplitude only) for a half-full tank are shown in Figure 13. Here again, the response is seen to possess a nonlinear softening characteristic, which is quite sensitive to excitation amplitude as had been intimated some time ago (4). However, the response curves are not very well defined in the areas of the jumps, as compared with those of the cylindrical tank, probably as a consequence of the increased tendency of breaking waves to form because of the curvature at the mean liquid level (breaking wave would not occur in the cylindrical tank at an equivalent wave amplitude). The breaking waves certainly have some tendency to modify the normal instability process in the region of the jump frequencies; nevertheless, the jump behavior has been approximately delineated in Figure 13 by the dashed lines. No liquid surface displacement or phase angle data were obtained for this tank configuration.

THEORETICAL CONSIDERATIONS
(Circular Cylindrical Tank)

In an effort to make some correlation between the foregoing experimental data and theoretical predictions, a careful review of available analyses was conducted. Of these, the theory developed by Hutton (3), for the circular cylindrical tank, appeared to offer most promise of being extended to yield appropriate force response information.

Brief Review of Hutton's Theory (3)

For a tank undergoing transverse oscillations, Hutton has assumed that the velocity potential of the disturbance can be approximated by the following simple form:

$$\hat{\phi} = \varepsilon^{\frac{1}{3}} \left[\psi_1(\xi,\tau) \cos(\omega t) + \chi_1(\xi,\tau) \sin(\omega t) \right]$$

$$+ \varepsilon^{\frac{2}{3}} \left[\psi_0(\xi,\tau) + \psi_2(\xi,\tau) \cos(2\omega t) + \chi_2(\xi,\tau) \sin(2\omega t) \right]$$

$$+ \varepsilon \left[\psi_3(\xi,\tau) \cos(3\omega t) + \chi_3(\xi,\tau) \sin(3\omega\tau) \right] \qquad (1)$$

where

$$t = \text{time}, \quad \tau = \tfrac{1}{2} \varepsilon^{\frac{2}{3}} \omega t, \quad \varepsilon = \omega \varepsilon_0$$

$$\omega = \text{frequency} \qquad (2a)$$

ε_o = tank displacement amplitude

$$\psi_1 = \left[f_1(\tau)\cos\theta + f_3(\tau)\sin\theta \right] J_1(\lambda_{11} r)\cosh(\lambda_{11}(z+h))/\cosh(\lambda_{11} h) \quad (2b)$$

$$\chi_1 = \left[f_2(\tau)\cos\theta + f_4(\tau)\sin\theta \right] J_1(\lambda_{11} r)\cosh(\lambda_{11}(z+h))/\cosh(\lambda_{11} h) \quad (2c)$$

$$\psi_0 = \text{constant} \quad (2d)$$

$$\psi_2 = \sum_{n=1}^{N} \hat{A}_{on} J_o(\lambda_{on} r)\cosh(\lambda_{on}(z+h))/\cosh(\lambda_{on} h) +$$
$$+ \sum_{n=1}^{N} \left(\hat{A}_{2n}\cos(2\theta) + \hat{B}_{2n}\sin(2\theta) \right) J_2(\lambda_{2n} r)\cosh(\lambda_{2n}(z+h))/\cosh(\lambda_{2n} h) \quad (2e)$$

$$\chi_2 = \sum_{n=1}^{N} \hat{C}_{on} J_o(\lambda_{on} r)\cosh(\lambda_{on}(z+h))/\cosh(\lambda_{on} h) +$$
$$+ \sum_{n=1}^{N} \left(\hat{C}_{2n}\cos(2\theta) + \hat{D}_{2n}\sin(2\theta) \right) J_2(\lambda_{2n} r)\cosh(\lambda_{2n}(z+h))/\cosh(\lambda_{2n} h) \quad (2f)$$

(N = 5 was used)

$$J_o'(\lambda_{on} a) = J_2'(\lambda_{2n} a) = J_1'(\lambda_{1n} a) = 0 \quad (2g)$$

The velocity potential is

$$\phi = \dot{x}_b r\cos\theta + \breve{\phi} \quad (3)$$

where x_b = tank displacement. The form of the disturbance potential, $\breve{\phi}$, in terms of $J_m(\lambda_{mn} r)\cosh(\lambda_{mn}(z+h))\begin{Bmatrix}\sin(m\theta)\\ \cos(m\theta)\end{Bmatrix}$ satisfies the Laplace equation for inviscid irrotational flow as well as the velocity potential. The coefficients were to be determined by a combined nonlinear free surface condition, to the third order.

First, by the method of expansion into the small parameter ε, the coefficients of $\varepsilon^{\frac{1}{3}}$, $\varepsilon^{\frac{2}{3}}$, ε must vanish for all times.

In doing so, the transformations

$$\tau = \frac{1}{2}\varepsilon^{2/3}\omega t \quad \text{and} \quad \rho_{11} = \omega^2(1-\nu\varepsilon^{2/3}) \tag{4a, b}$$

were introduced.

For the $\varepsilon^{1/3}$ term to vanish, the conditions are satisfied by the assumed forms of ψ_1 and χ_1 . The $\varepsilon^{2/3}$ term contains only the constant term and the second harmonics. There were three resultant equations which are satisfied by the Galerkin method (or in this case the Fourier-Bessel technique), with the assumed forms of ψ_0, ψ_2, χ_2. This determines $\hat{A}_{0n}$, $\hat{A}_{2n}$, $\hat{B}_{2n}$, $\hat{C}_{0n}$, $\hat{C}_{2n}$, $\hat{D}_{2n}$ in terms of f_i. It is noted that the equation resulting from terms independent of time is satisfied by ψ_0 = constant and that the remaining two equations yield six equations from their components in J_0 , $J_2\cos(2\theta)$, $J_2\sin(2\theta)$

In the ε term, however, only the two first harmonic terms were assumed to vanish, treating time derivatives as constants. Their $J_1\sin\theta$ and $J_1\cos\theta$ components yield a set of four first-order nonlinear differential equations governing (i = 1, 2, 3, 4). This set of equations determines both the steady-state harmonic solution (when the amplitude does not change with time) and the stability boundary (when f_i varies as $c_i e^{\lambda t}$ + steady state value of f_i ; c_i small).

Force on the Tank*

The pressure is given by Bernoulli's equation in terms of the disturbance potential, as

$$p = -\rho\left\{ \frac{\partial \breve{\phi}}{\partial t} + g z + \frac{1}{2}(\nabla \breve{\phi} \cdot \nabla \breve{\phi}) + \ddot{x}_1 r\cos\theta + \cancel{f(t)}^{\,0} \right\} + p_0 \qquad (5)$$

where an arbitrary function of time $f(t)$ can be absorbed into $\frac{\partial \breve{\phi}}{\partial t}$ through a redefinition of $\breve{\phi}$.

The x-force on the tank is given by

$$F_x = \left[\int_{-h}^{\eta} \int_{0}^{2\pi} p\, a \cos\theta \, d\theta \, dz \right]_{r=a}$$

where η is the free surface elevation, a is the radius of the rigid tank, and h is the (initial) liquid depth. F_x can be evaluated to the third order, consistent with Hutton's theory (3), except for the contributions due to ψ_3 and χ_3 which were not originally derived. Thus,

$$F_x \doteq F_1 + F_2 \qquad (6)^*$$

where:

$$F_1 = \left[\int_{-h}^{0} \int_{0}^{2\pi} p\, a \cos\theta \, d\theta \, dz \right]_{r=a} =$$

*These force expressions were first derived by Dr. Kishor Doshi of SwRI.

$$= F_1 = -\rho a \left\{ -\varepsilon^{\frac{1}{3}} \omega \sin(\omega t) \frac{A\pi \sinh(\lambda_{11} h)}{\lambda_{11}} + \frac{\varepsilon}{2a^2} \left(\sin(\omega t) + \sin(3\omega t) \right) \cdot \right.$$

$$\cdot \sum_{n=1}^{\infty} \frac{\pi}{2} A_\theta \frac{N_\theta}{(\lambda_{11}^2 - \lambda_{2n}^2)} \left[\lambda_{11} \sinh(\lambda_{11} h) \cosh(\lambda_{2n} h) - \lambda_{2n} \cosh(\lambda_{11} h) \cdot \right.$$

$$\left. \cdot \sinh(\lambda_{2n} h) \right] + \frac{\varepsilon}{2} \left[\sin(\omega t) + \sin(3\omega t) \right] \cdot \sum_{n=1}^{\infty} \frac{\pi}{2} A_z \left[\frac{2M_z}{(\lambda_{11}^2 - \lambda_{on}^2)} \left[\lambda_{11} \cdot \right. \right.$$

$$\left. \cdot \cosh(\lambda_{11} h) \sinh(\lambda_{on} h) - \lambda_{on} \sinh(\lambda_{11} h) \cosh(\lambda_{on} h) \right] + \frac{N_z}{(\lambda_{11}^2 - \lambda_{2n}^2)} \left[\lambda_{11} \cosh(\lambda_{11} h) \cdot \right.$$

$$\left. \left. \left. \cdot \sinh(\lambda_{2n} h) - \lambda_{2n} \sinh(\lambda_{11} h) \cosh(\lambda_{2n} h) \right] \right] - \varepsilon \omega a \pi h \sin(\omega t) \right\} \quad (6a)$$

and

$$F_2 = \left[\int_0^{\eta} \int_0^{2\pi} p\, a \cos\theta \, dz \right]_{r=a}$$

$$= -\int_0^{2\pi} a \left[\eta\, p(a,\theta,0) + \frac{\eta^2}{2} p_z(a,\theta,0) + O(\eta^4) \right] \cos\theta \, d\theta$$

$$\overset{u}{=} -\int_0^{2\pi} \left[\frac{-p^2(a,\theta,0)}{p_z(a,\theta,0)} + \frac{1}{2} \frac{p^2(a,\theta,0)}{p_z(a,\theta,0)} \right] a \cos\theta \, d\theta$$

$$= \int_0^{2\pi} \frac{1}{2} \frac{p^2}{p_z} a \cos\theta \, d\theta =$$

$$= F_2 = \frac{1}{2}\frac{\rho a}{g}\pi\varepsilon\left\{\frac{3}{4}\frac{\omega^3}{g}\sin^3(\omega t)\left[\gamma J_1(\lambda_{11}a)\right]^3\lambda_{11}\tanh(\lambda_{11}h) - \right.$$

$$-4\omega^2\sin(\omega t)\cos(2\omega t)\left[\gamma J_1(\lambda_{11}a)\left[\sum_{n=1}^{\infty}\hat{C}_{on}J_0(\lambda_{on}a) + \right.\right.$$

$$\left.\left. + \frac{1}{2}\sum_{n=1}^{\infty}\hat{C}_{2n}J_2(\lambda_{2n}a)\right]\right] - \left[\frac{\omega}{a^2}\frac{\sin(\omega t)}{4}\left(\frac{1+\cos(2\omega t)}{2}\right)\left[\gamma J_1(\lambda_{11}a)\right]^3\right]$$

$$\left. - \left[\frac{3}{4}\omega\sin(\omega t)\left(\frac{1+\cos(2\omega t)}{2}\right)\right]\left[\left[\gamma J_1(\lambda_{11}a)\right]^3\left[\lambda_{11}\tanh(\lambda_{11}a)\right]^2\right]\right\} \quad (6b)^*$$

where

$$M_z = \hat{C}_{on}\frac{\lambda_{on}J_0(\lambda_{on}a)}{\cosh(\lambda_{on}h)} \quad (7a)$$

$$N_\theta = -2\frac{\hat{C}_{2n}J_2(\lambda_{2n}a)}{\cosh(\lambda_{2n}h)} \quad (7b)$$

$$N_z = \lambda_{2n}\frac{\hat{C}_{2n}J_2(\lambda_{2n}a)}{\cosh(\lambda_{2n}h)} \quad (7c)$$

$$A = \frac{\gamma J_1(\lambda_{11}a)}{\cosh(\lambda_{11}h)} \quad (7d)$$

$$A_\theta = -A \quad (7e)$$

$$A_z = \lambda_{11}A \quad (7f)$$

$$\hat{C}_{on} = -\frac{\gamma^2}{2}\Omega_{on} \quad (7g)$$

---

*The relation $\eta \stackrel{\wedge}{=} \frac{-\hbar(r,\theta,0)}{\hbar_z(r,\theta,0)}$ has been utilized in deriving F_2.

$$\hat{C}_{2n} = -\frac{\gamma^2}{2}\,\Omega_{2n} \tag{7h}$$

Ω_{0n}, Ω_{2n} are given by Hutton (3). γ is the amplitude of the steady-state part of f_1, and is governed by a cubic equation depending on the motion being planar or nonplanar*.

Results

As described and discussed previously, total force response data calculated from the foregoing theory have been compared with relevant experimental data in Figure 9.

*Through private communications with Dr. Hutton, it was learned that I_{q3}^{n} in the expressions for $\hat{G}_1$ and $\hat{G}_2$ should be replaced by $I_{q3}^{n} / \lambda_{11}^{2}$, in order to calculate γ correctly.

CONCLUSIONS AND RECOMMENDATIONS

This study of some of the gross nonlinear characteristics of lateral sloshing in rigid containers, exploratory though it was, has revealed a number of important and interesting features. While the character of the force response in circular cylindrical and spherical tanks may have been entirely as anticipated, that in sector compartmented tanks certainly was not. In fact, the phasing of forces between sectors led to a total response picture of somewhat unique nature. The continued use of compartmented tanks in actual vehicle design would certainly indicate the desirability of further investigations along these lines.

Theoretical developments are woefully lacking. Even the best available theory for the circular cylindrical tank is quite poor, except for the in-phase branch at low amplitudes. Efforts to develop a nonlinear theory for the sector compartmented tank should be initiated as promptly as possible.

ACKNOWLEDGEMENTS

The authors are very much indebted to J. E. Modisette for performing most of the experiments and analyzing the data, with the assistance of R. B. Stiles; to P. S. Westine and R. Gonzales for performing some analyses and many computations; and to V. Hernandez for preparing the figures.

REFERENCES

1. Abramson, H. N., "Dynamic Behavior of Liquids in Moving Containers," Applied Mechanics Reviews, 16, 7, pp. 501-506, July 1963.

2. Berlot, R. R., "Production of Rotation in a Confined Liquid Through Translational Motions of the Boundaries," Journal of Applied Mechanics, 26, 4, pp. 513-516, December 1959.

3. Hutton, R. E., "An Investigation of Nonlinear, Nonplanar Oscillations of Fluid in a Cylindrical Container," NASA Tech. Note D-1870 (May 1963).

4. Abramson, H. N., Chu, W. H., and Garza, L. R., "Liquid Sloshing in Spherical Tanks," AIAA Journal, 1, 2, pp. 384-389, February 1963.

5. Abramson, H. N., Garza, L. R., and Kana, D. D., "Liquid Sloshing in Compartmented Cylindrical Tanks," ARS Journal, 32, 6, pp. 978-980, June 1962.

6. Abramson, H. N., and Garza, L. R. "Some Measurements of Liquid Frequencies and Damping in Compartmented Cylindrical Tanks," AIAA Journal of Spacecraft and Rockets, to appear.

7. Dalzell, J. F., Chu, W. H., and Modisette, J. E., "Studies of Ship Roll Stabilization Tanks," Tech. Rept. No. 1, Contract Nonr-3926(00), Southwest Research Institute, August 1964.

8. Dodge, F. T., Kana, D. D., and Abramson, H. N., "Liquid Surface Oscillations in Longitudinally Excited Rigid Cylindrical Containers," AIAA Technical Paper 65-83 (also, AIAA Journal, in press).

9. Lindholm, U. S., Kana, D. D., and Abramson, H. N., "Breathing Vibrations of a Circular Cylindrical Shell with an Internal Liquid," Journal of the Aerospace Sciences, 29, 9, pp. 1052-1059, September 1962.

10. Kana, D. D., Lindholm, U. S., and Abramson, H. N., "An Experimental Study of Liquid Instability in a Vibrating Elastic Tank," Tech. Rept. No. 5, Contract NASw-146, Southwest Research Institute, January 1963.

11. Abramson, H. N., and Ransleben, G. E., Jr., "Simulation of Fuel Sloshing Characteristics in Missile Tanks by Use of Small Models," ARS Journal, 30, 7, pp. 603-612, July 1960.

12. Kana, D. D., "A Resistive Wheatstone Bridge Liquid Wave Height Transducer," Tech. Rept. No. 3, Contract NAS8-11045, Southwest Research Institute, May 1964.

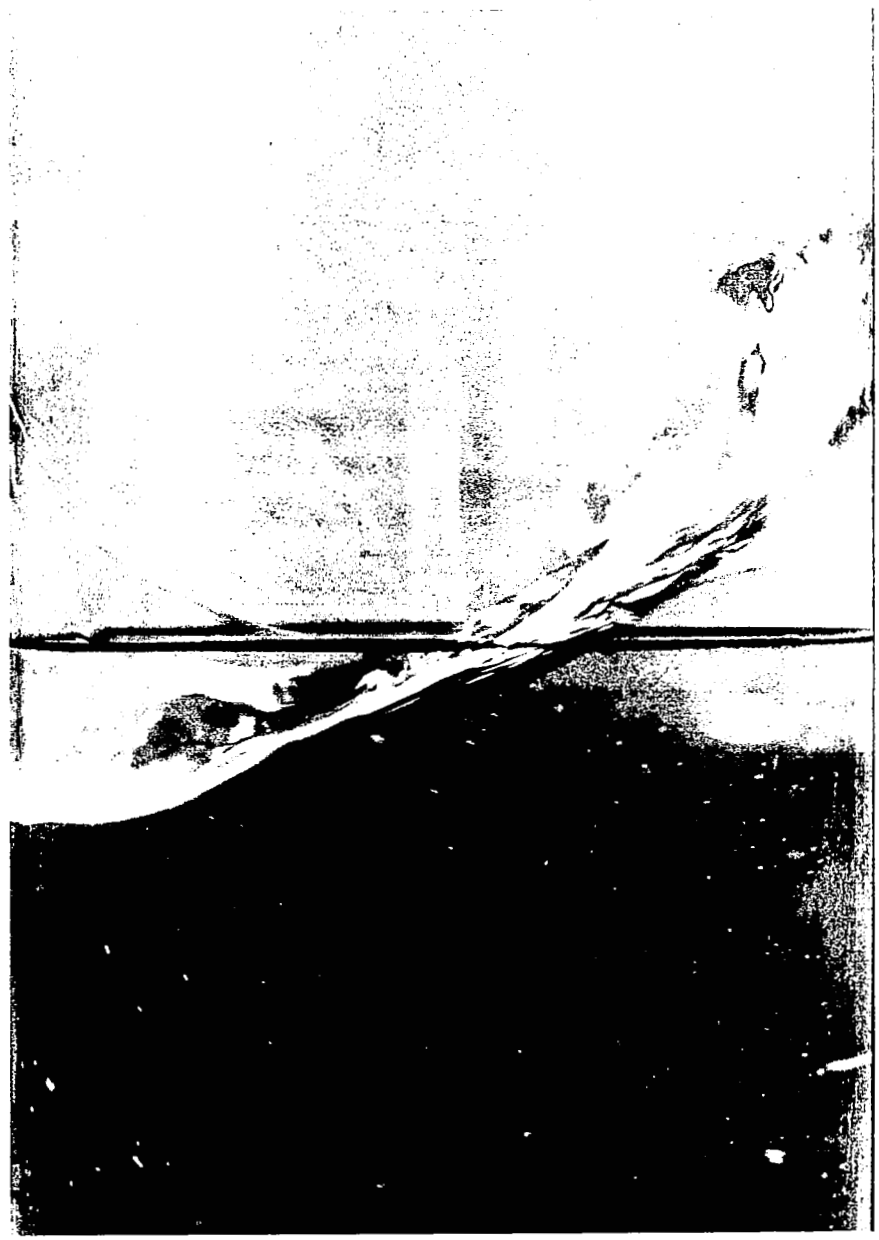

FIGURE I. LARGE AMPLITUDE BREAKING WAVE DURING LATERAL SLOSHING NEAR FIRST MODE RESONANCE

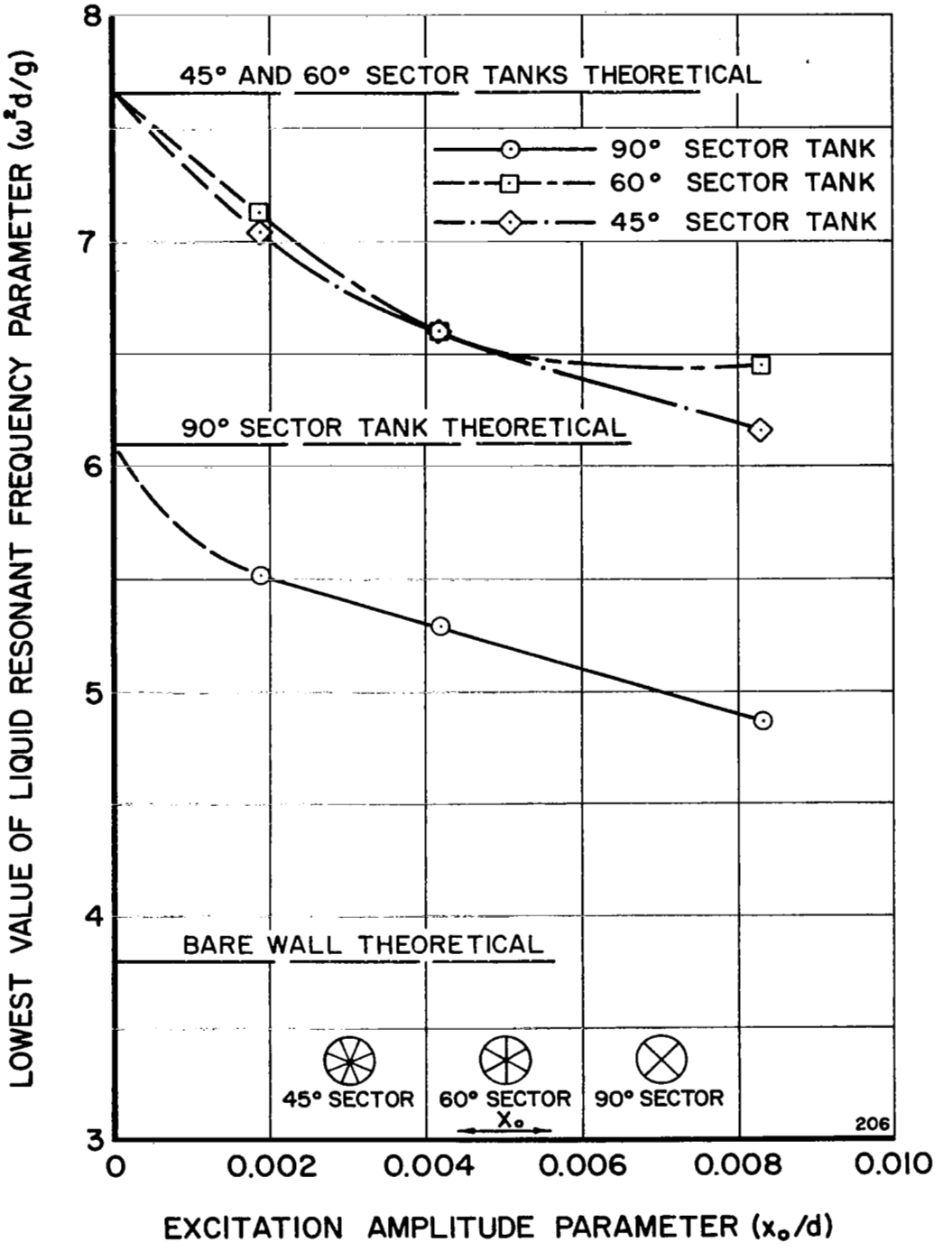

FIGURE 2. EFFECT OF EXCITATION AMPLITUDE ON THE LOWEST RESONANT FREQUENCY FOR 45°, 60°, AND 90° SECTORED CYLINDRICAL TANKS

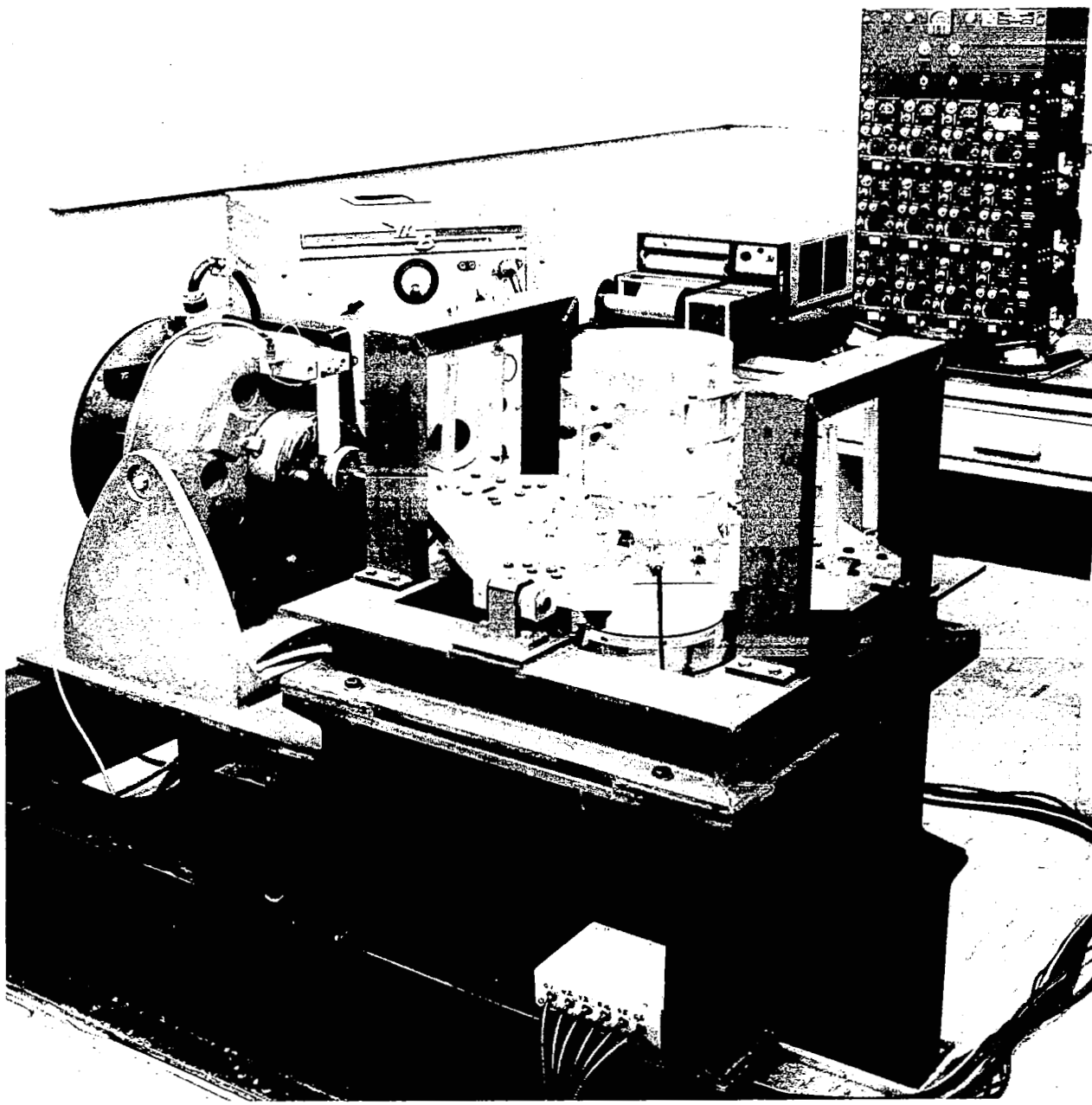

FIGURE 3. EXPERIMENTAL APPARATUS FOR LATERAL SLOSHING

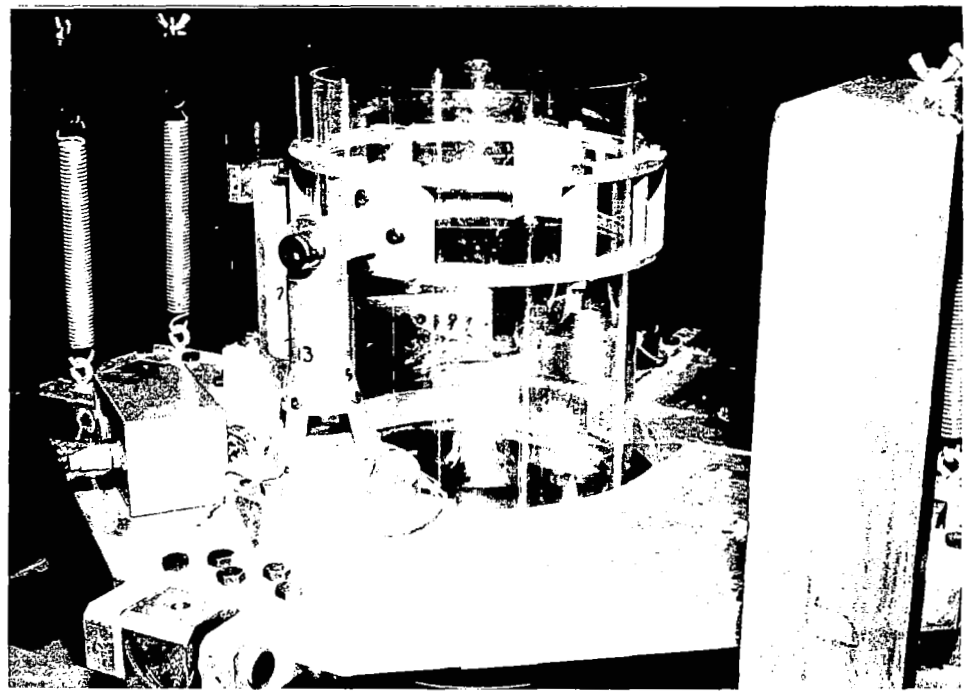

(a) CYLINDRICAL TANK

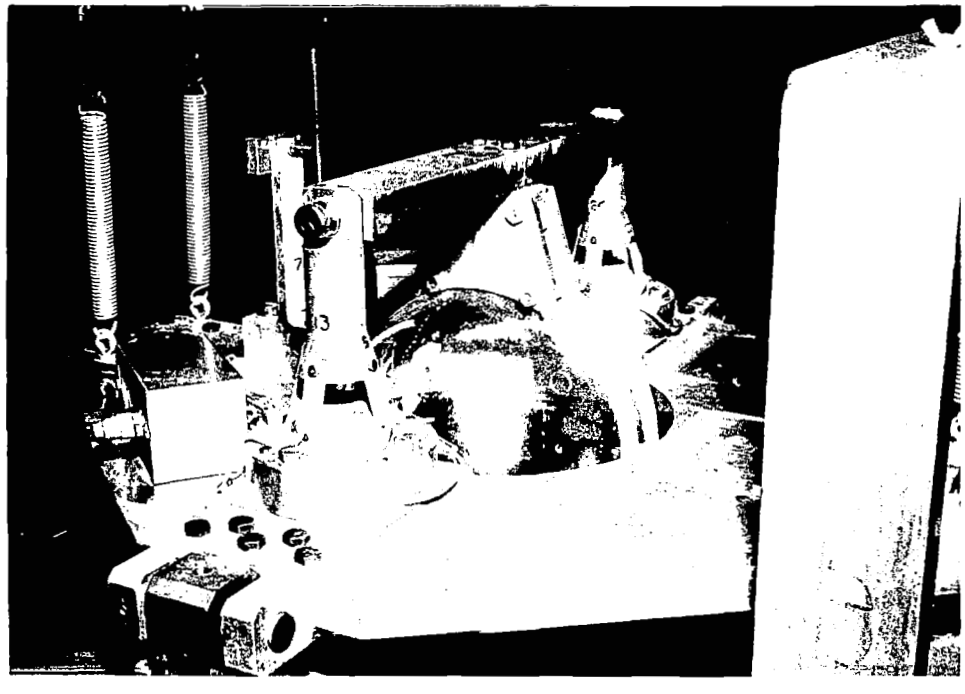

(b) SPHERICAL TANK

FIGURE 4. MOUNTING DETAILS OF TANKS IN TEST APPARATUS

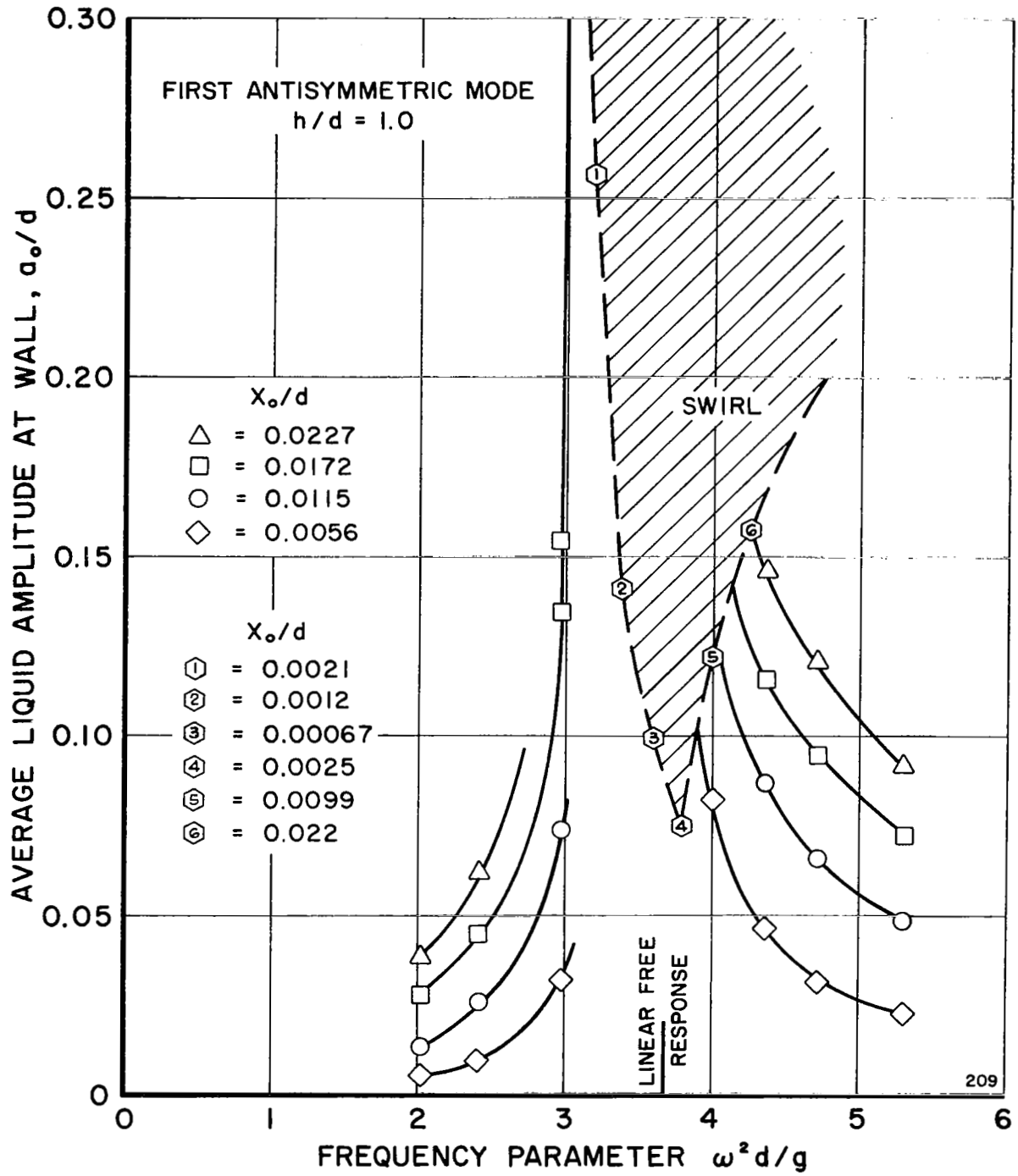

FIGURE 5. LIQUID FREE SURFACE RESPONSE IN CIRCULAR CYLINDRICAL TANK SHOWING SWIRL REGION

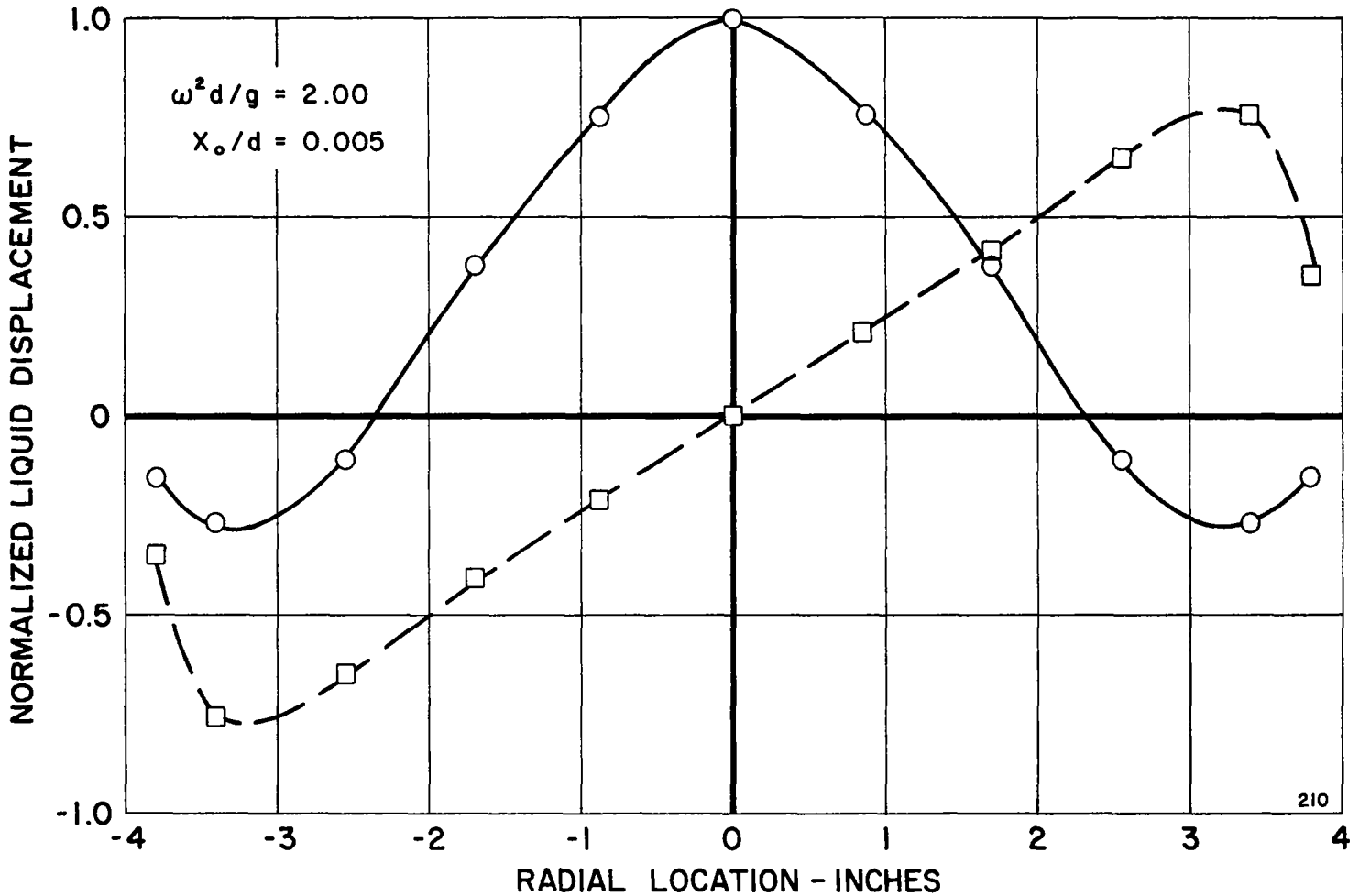

FIGURE 6. SYMMETRIC AND ANTISYMMETRIC COMPONENTS OF LIQUID SURFACE DISPLACEMENT IN CIRCULAR CYLINDRICAL TANK

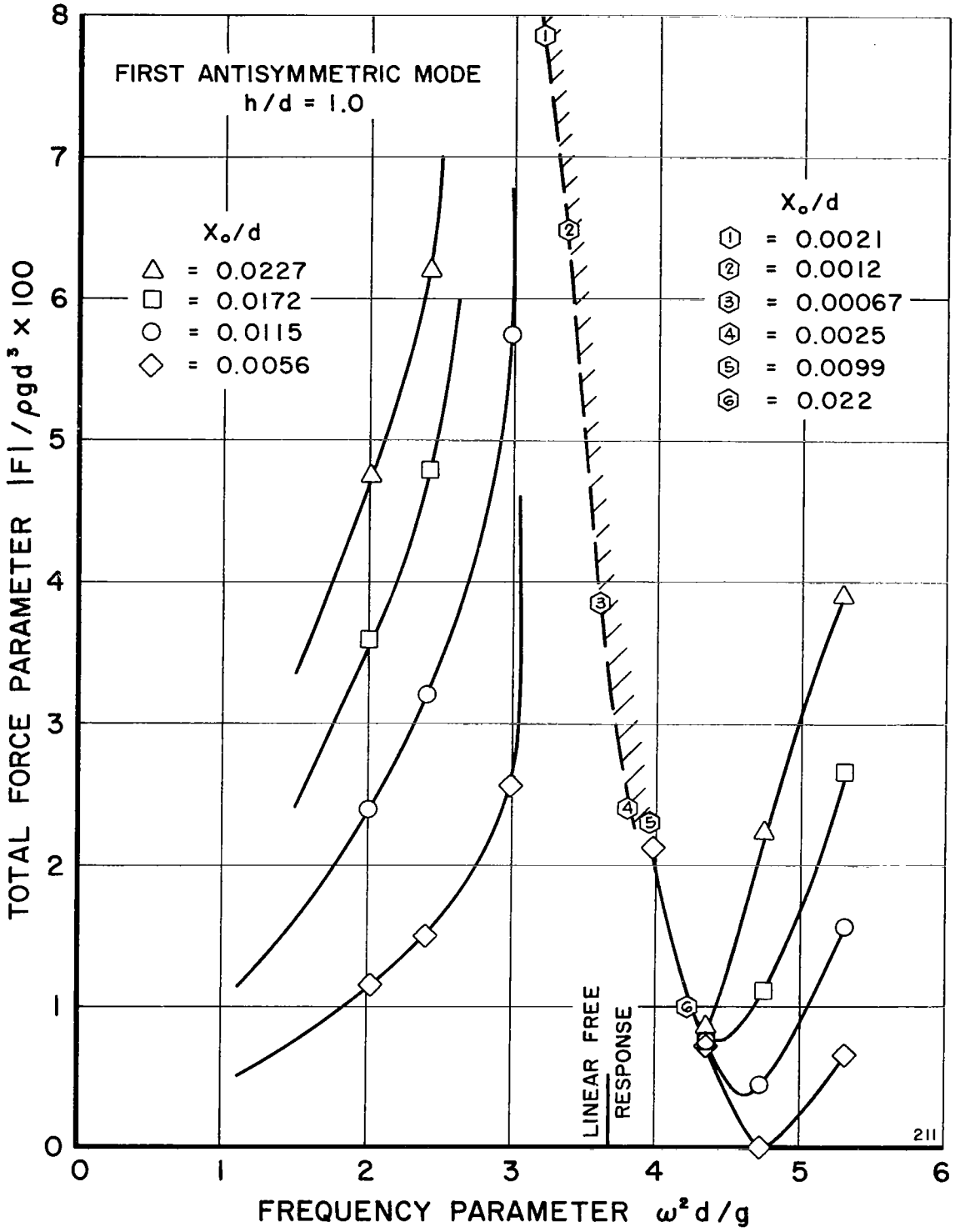

FIGURE 7. LIQUID FORCE RESPONSE IN CIRCULAR CYLINDRICAL TANK

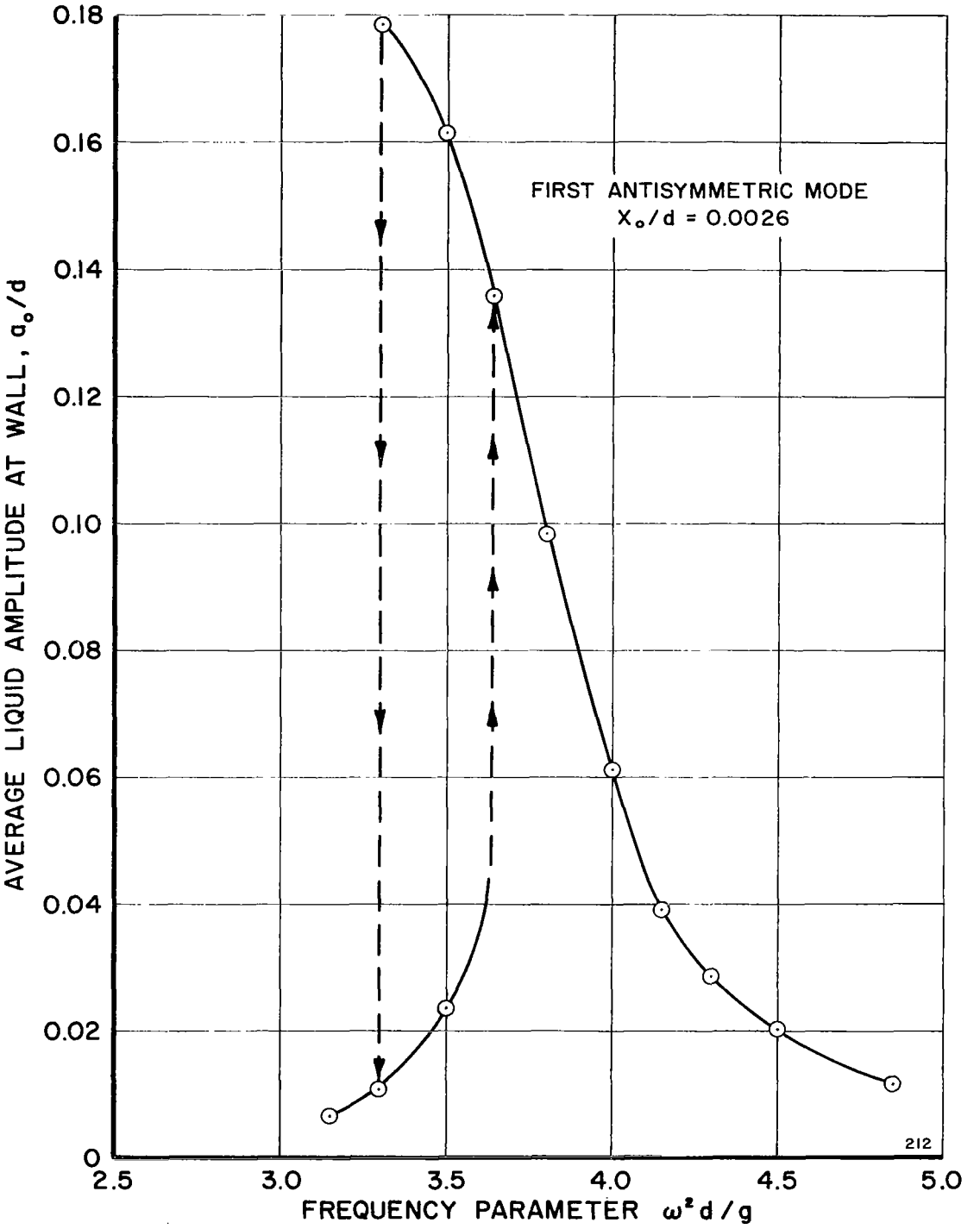

FIGURE 8. LIQUID FREE SURFACE RESPONSE IN HALF-CYLINDRICAL TANK DEMONSTRATING NONLINEAR CHARACTERISTICS

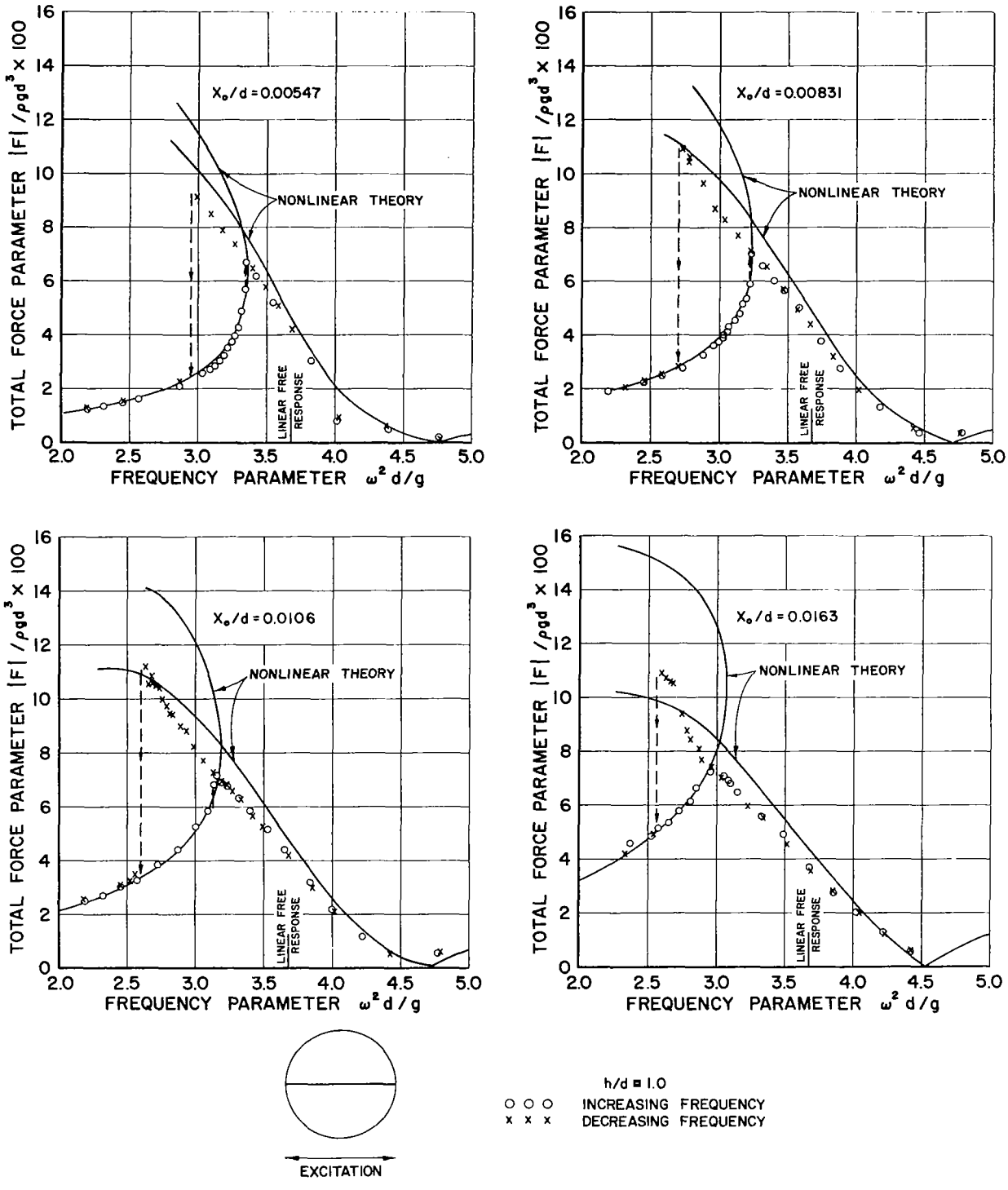

FIGURE 9. AMPLITUDE OF LIQUID FORCE RESPONSE IN HALF-CYLINDRICAL TANK

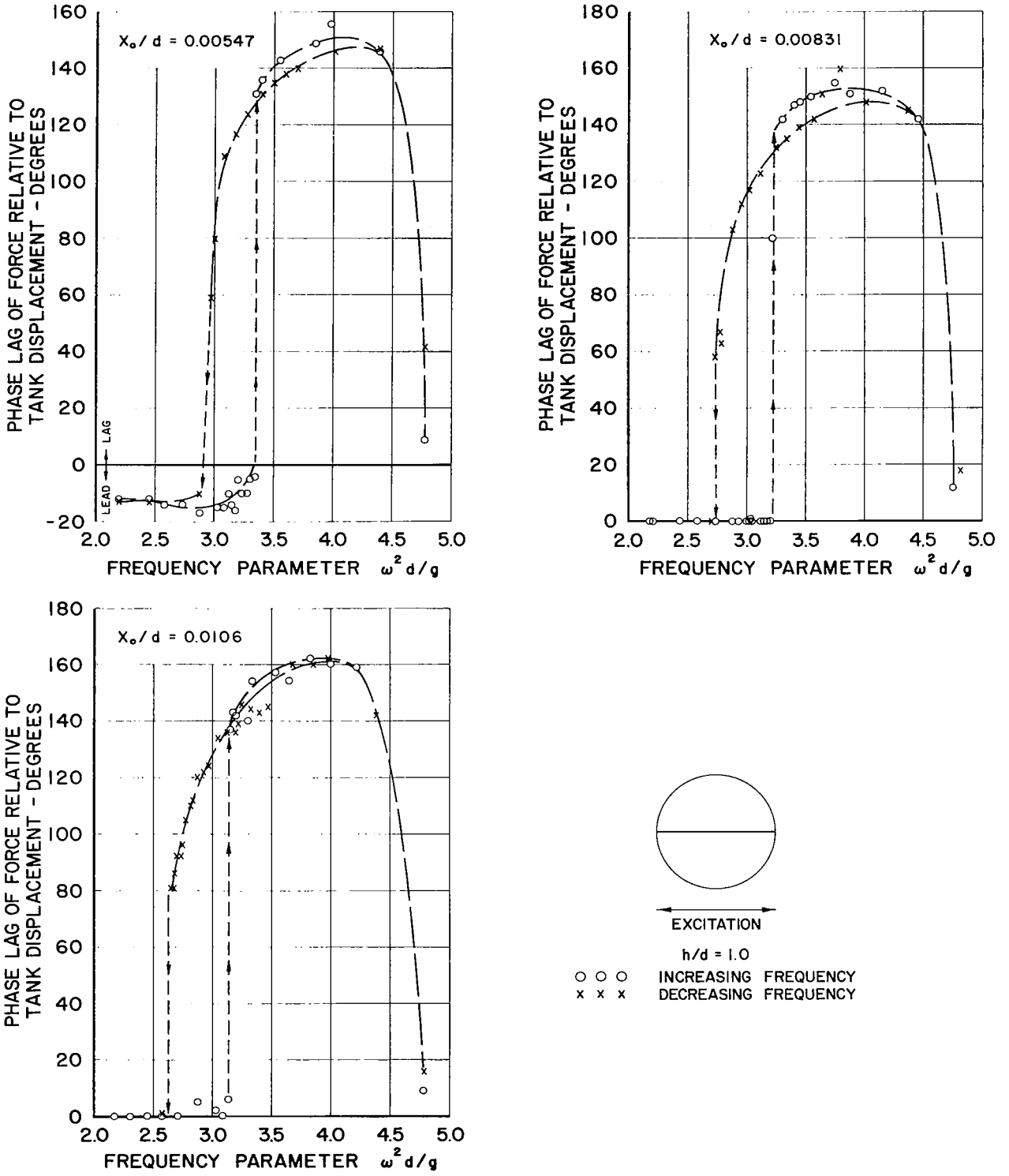

FIGURE 10. PHASE ANGLE OF LIQUID FORCE RESPONSE IN HALF-CYLINDRICAL TANK

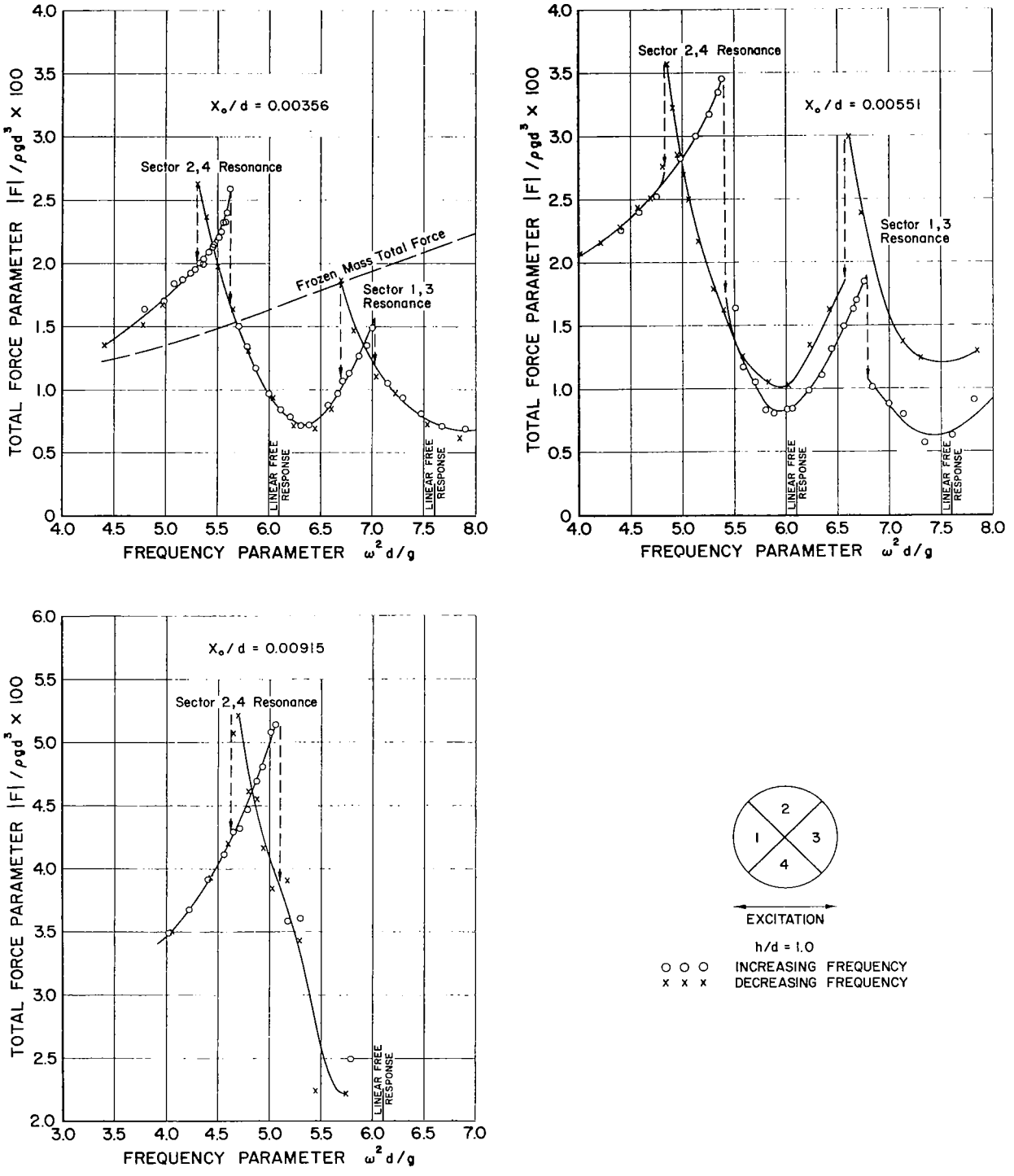

FIGURE 11. AMPLITUDE OF LIQUID FORCE RESPONSE IN 90° SECTOR CYLINDRICAL TANK

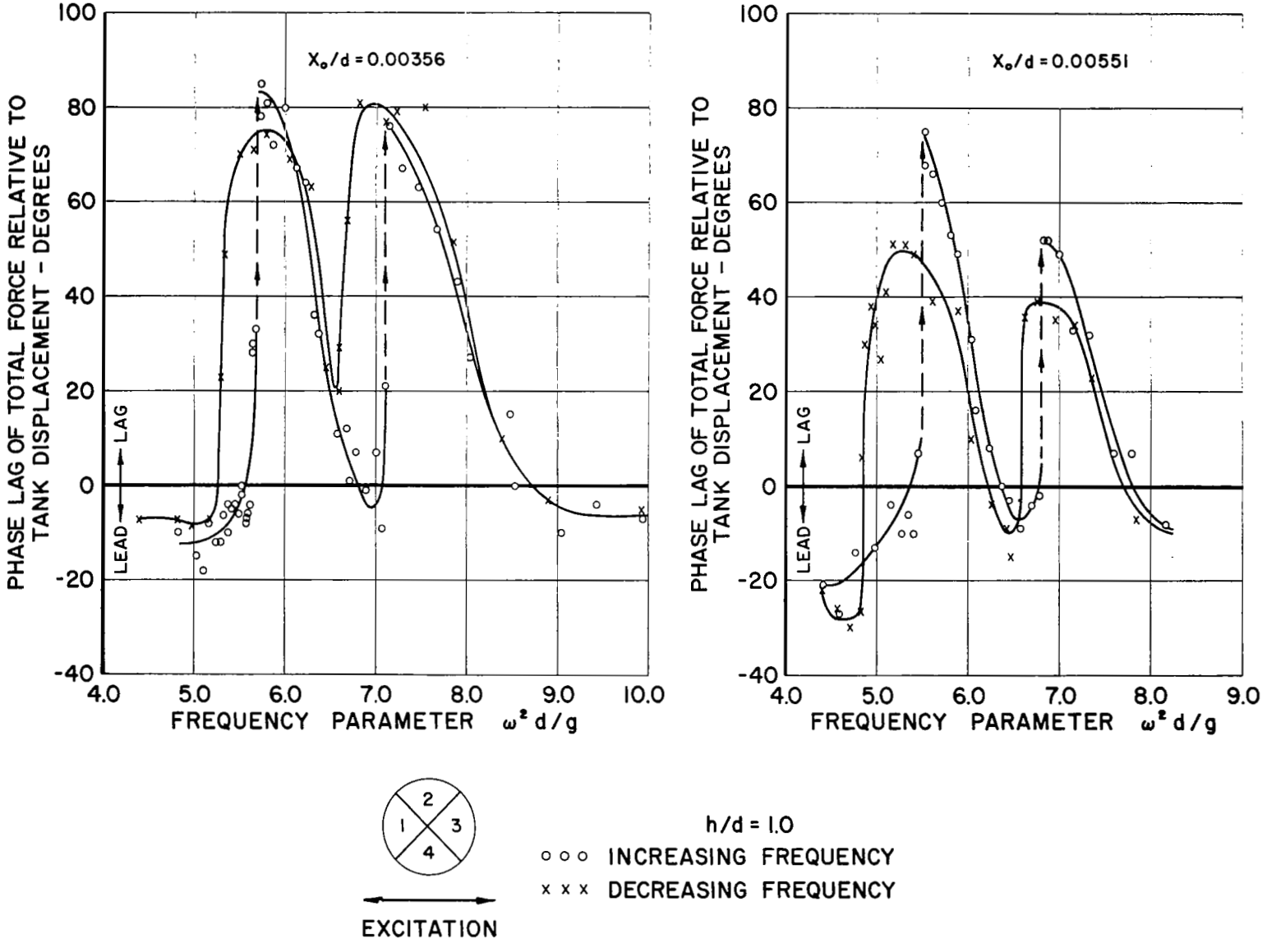

FIGURE 12. PHASE ANGLE OF LIQUID FORCE RESPONSE IN 90° SECTOR CYLINDRICAL TANK

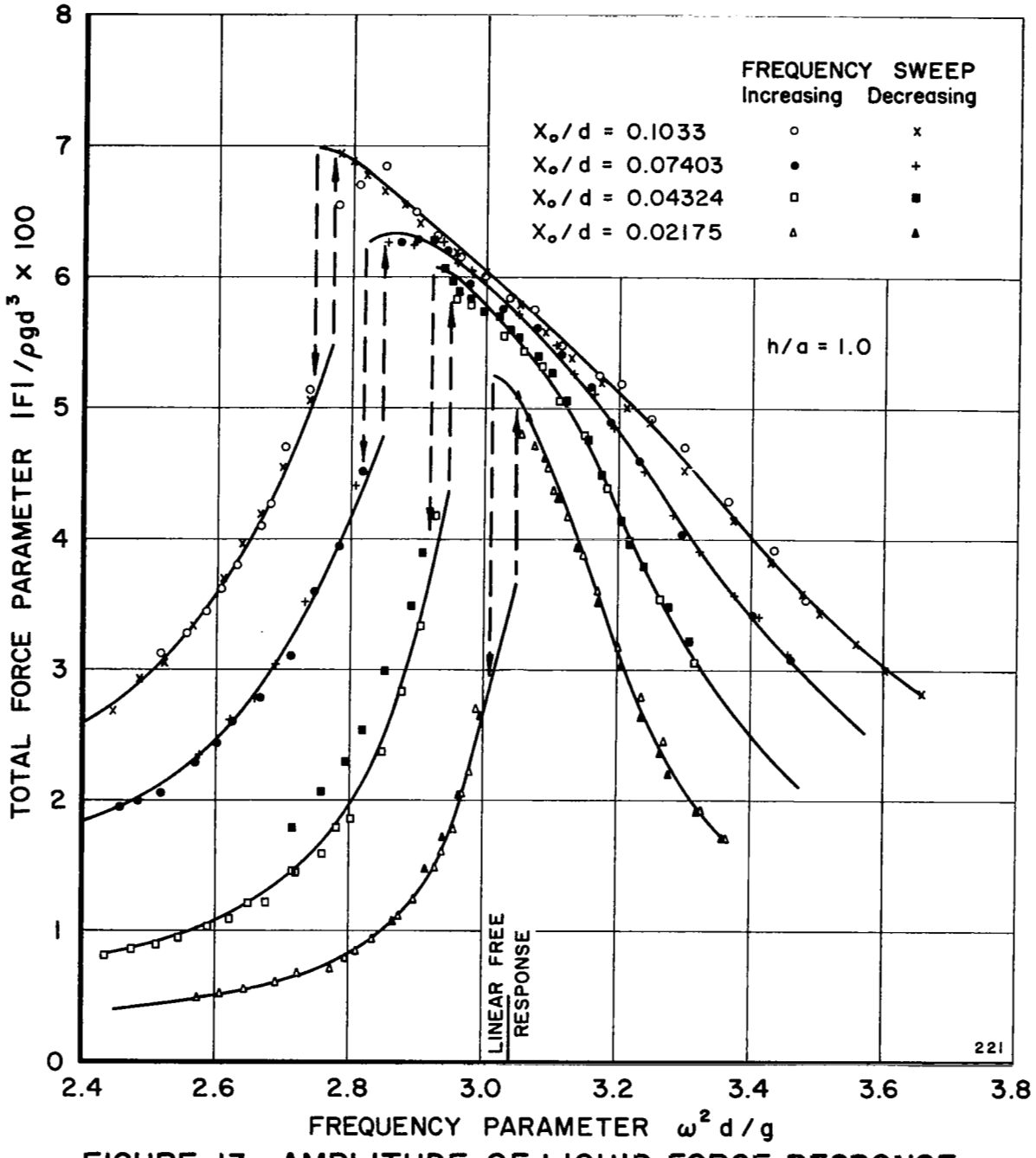

FIGURE 13. AMPLITUDE OF LIQUID FORCE RESPONSE IN SPHERICAL TANK